Effect of Al, Cu, Ga, and Nb additions on the magnetic properties and microstructural features of sintered NdFeB

S. Pandian, V. Chandrasekaran, G. Markandeyulu, K. J. L. Iyer, and K. V. S. Rama Rao

Citation: Journal of Applied Physics **92**, 6082 (2002); doi: 10.1063/1.1513879
View online: http://dx.doi.org/10.1063/1.1513879
View Table of Contents: http://scitation.aip.org/content/aip/journal/jap/92/10?ver=pdfcov
Published by the AIP Publishing

Effect of Al, Cu, Ga, and Nb additions on the magnetic properties and microstructural features of sintered NdFeB

S. Pandian and V. Chandrasekaran
Defence Metallurgical Research Laboratory, Hyderabad - 500 058, India

G. Markandeyulu, K. J. L. Iyer, and K. V. S. Rama Rao[a)]
Indian Institute of Technology Madras, Chennai - 600 036, India

(Received 20 May 2002; accepted 21 August 2002)

This study describes the relative effect on the permanent magnet characteristics viz. remanence (B_r), intrinsic coercivity (H_{ci}), Curie temperature (T_C), and rectangularity of the intrinsic demagnetization curve, when Al, Cu, Ga, and Nb are added individually to NdFeB. Each elemental addition causes significant improvement in H_{ci} but the level of improvement differs from one additive element to the other. The addition of Nb is favored over other elements for realizing maximum enhancement in H_{ci} and rectangularity of the demagnetization curve. The microstructural features of the sintered samples of NdFeB with elemental addition show the formation of a new phase, in addition to the phases (φ, η, and Nd-rich) generally found in the ternary sample. The factors influencing the permanent magnet characteristics of sintered samples are the distribution of the Nd-rich phase in the intergranular region, the size and distribution of the minor phases at the grain junctions, the formation and distribution of new phases due to alloying addition, and the solubility of the dopant element in various phases coexisting in the sample. © *2002 American Institute of Physics.* [DOI: 10.1063/1.1513879]

I. INTRODUCTION

High energy density sintered NdFeB magnets have been receiving much attention of researchers for quite a long time for its excellent device miniaturization, which hitherto was never visualized as feasible with other classes of permanent magnet materials. The low Curie temperature ($T_C \sim 585$ K) of the compound $Nd_2Fe_{14}B$ (φ phase) has, however, become a matter of concern. The consequence of this deficiency is reflected in the temperature coefficient of remanence (B_r) and intrinsic coercivity (H_{ci}), especially in the latter.[1] Alloying additions selectively improve some properties but affect the other. For example, partial substitution of Fe by Co results in increasing the T_C but reducing the H_{ci} [2–4] and that of Nd by Dy results in increasing the magnetocrystalline anisotropy (H_A) but reducing the B_r. [5–7] Coercivity in sintered NdFeB magnets has a strong dependence on the microstructure. One of the phase constituents in the NdFeB magnet is a low melting (928 K) eutectic Nd-rich phase, which acts as a sintering aid liquid phase. The distribution of it as a thin layer (~ 2 nm) separating the grains of the hard magnetic phase (φ) is considered a unique microstructural feature that brings significant enhancement in H_{ci}. The micromagnetism modeling studies proposed a phenomenological equation linking H_{ci} and microstructural parameters.[8–10] Al or Ga is known to cause significant improvement in H_{ci}, which is attributed to the better distribution of the Nd-rich intergranular phase with the solubility of the additive element in it.[11–14] Recently, we reported that different intergranular phases formed with Al and spread of the Nd-rich phase at the grain junctions seem to be the microstructural factors that limit the value of H_{ci} beyond a certain Al concentration level in the alloy.[15] The minor addition of elements such as Nb or Cu is also known to bring enhancement in coercivity.[16,17] For the realization of concomitant improvement in the second quadrant characteristics and in the thermomagnetic characteristics of the magnet for elevated temperature performance, an optimal combination of elemental additions such as Dy, Co as the main, and Al, Cu, Ga, Nb, etc. as the minor have been found to be suitable.[18–21] Our recent paper describes that simultaneous addition of Dy, Co, Ga, Cu, and Nb is gainful to increase both H_{ci} and T_C of ternary NdFeB.[22] The enhancement in the properties has been attributed to the distribution of the additive elements in the various phases as to cause maximum beneficial effect on some property while marginalizing their deleterious effect on the other properties. NdFeB magnets for moderate temperature applications, however, may not require the addition of expensive elements Co and Dy if high H_{ci} and a near rectangular intrinsic demagnetization curve can be realized with elemental additions such as Al, Cu, Ga, Nb, etc. The information on the comparative study to make a qualitative assessment on the development of magnetic properties and to bring out relative merits of each elemental addition to NdFeB is rather limited. In the present study, an attempt has been made to interrelate the second quadrant characteristics with the microstructural features arising out of each addition of Al, Cu, Ga, and Nb. Since the ultimate properties obtained in sintered magnets depend critically on the composition of the alloy, its powder characteristics, and thermal and other process parameters, identical conditions were maintained for the study of each alloying addition to establish a reliable comparison.

a)Electronic mail: kvs@physics.iitm.ac.in

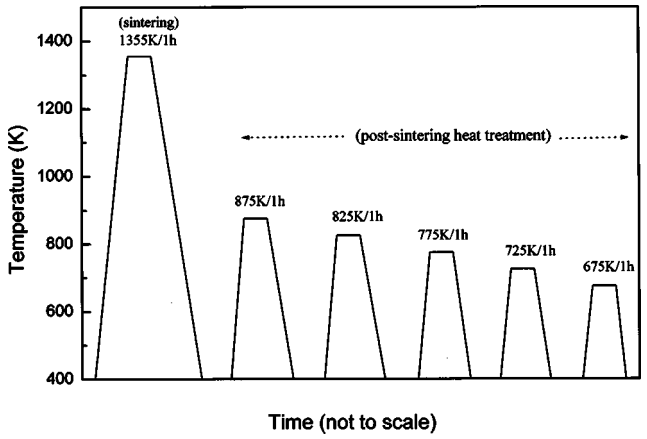

FIG. 1. Sintering and postsintering heat treatment schedule adopted for NdFeB samples.

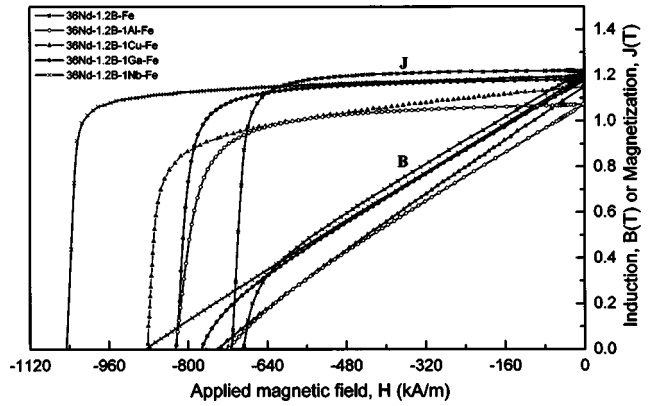

FIG. 2. Second quadrant hysteresis loop of sintered alloys, heat treated to achieve peak values of H_{ci}.

II. EXPERIMENT

Alloys of nominal composition 36Nd–1.2B–Fe and 36Nd–1.2B–1.0M–Fe, where M=Al, Cu, Ga, or Nb, were prepared by melting the high purity elements (Nd, Dy, Co, Al, Nb, Cu; 99.9% and B, Ga; 99.5%) under vacuum and chill casting the alloy in a copper mold. The as-cast alloy obtained in plate form was reduced to powder of average particle size $\sim 5\ \mu$m by ball milling for 1.5 h. The powders were compacted into cylindrical samples of 20 mm diameter and 10 mm height in a nonmagnetic die under the simultaneous application of a magnetic field of strength 1.5 T and compacting pressure of 240 MPa. The powder compacts have been sintered at 1355 K for 1 h followed by a postsintering heat treatment at an intermediate temperature range 875 – 675 K. The treatment schedule adopted for the samples is described in Fig. 1.

Using the autohysteresis loop tracer (M/s Walker Scientific Inc.) the second quadrant hysteresis curves were plotted for the samples after each thermal treatment. Thermomagnetic plots with an applied field of $H=0.02$ T were made using a vibrating sample magnetometer (M/s Digital Measurement Systems). X-ray diffraction patterns of the samples have been taken using a Philips diffractometer. The microstructural features of the samples have been investigated with the help of optical metallography and EPMA (CAMECA electron probe microanalysis). A solution of 2% Nital was used as an etchant to reveal the microstructural features of the samples.

III. RESULTS AND DISCUSSION

The normal and intrinsic demagnetization curves of the samples heat treated to obtain peak coercivity are shown in Fig. 2, while B_r, H_{ci}, and T_C are compared in Table I. It has been observed that every additive element causes significant improvement in H_{ci} over that realized in the ternary composition. A marginal reduction in B_r of about 2% to 3% is observed in the case of Nb and Ga additions. However, with Al and Cu addition a significant fall of 5%–10% is observed. The peak coercivity value measured in a sample with Nb additive is about 20% higher than that measured in samples with the addition of Al, Ga, or Cu. The rectangularity of the intrinsic demagnetization curve, assessed from the ratio of H_k/H_{ci}, where H_k is the knee field required to bring 10% reduction in B with respect to B_r, is found to be better with Nb or Ga addition as compared to that of Al or Cu addition.

H_{ci} values of the samples measured after each heat treatment are shown in Fig. 3. The peak H_{ci} value has been realized with a postsintering heat treatment of 875 K for 1 h in all alloy samples except in the sample with Nb addition. The H_{ci} enhancement from the sintered to heattreated condition is observed to be of 20%–25% in ternary and in samples with additive elements of Al or Cu. In the case of Ga and Nb added samples, the trend was found to be different. The H_{ci} value measured in the as-sintered condition for a Ga added sample has been the lowest (430 kA/m) and the enhancement is almost double after the heat treatment at 875 K for 1 h.

In the Nb added sample, a progressive improvement in H_{ci} during the step-heat treatment from 875 to 775 K takes place, which can be attributed to the microstructural effect that will be discussed later.

The thermomagnetic plots of the samples are shown in Fig. 4. There is no evidence of the existence of any other ferromagnetic phase having T_C less than that of the φ phase ($Nd_2Fe_{14}B$). The T_C of the φ phase corresponding to each alloy composition is shown in Table I. Al and Cu cause noticeable reduction in T_C, while Nb causes minimal dilution. With Ga, however, a marginal increase in T_C was observed which is in agreement with an earlier report[23] for low concentration additions of Ga. The magnetization is negligibly small after the crossover of the T_C of the φ phase in all the samples with additives. A significant value of magnetization, however, remains in the ternary NdFeB sample, indicating the presence of residual Fe in the sample.

X-ray diffraction patterns of the sintered samples, with the sample surface exposed to an x-ray perpendicular to the direction of the texture axis, are shown in Fig. 5. The optical micrographs of the samples are shown in Fig 6. The micrographs show the presence of three phases viz., φ as the main and η and Nd-rich as minor phases in all the samples. An additional minor phase is found formed in doped samples. The minor phases are found to be distributed at the grain

TABLE I. Comparison of magnetic properties (B_r, H_{ci}, H_k, T_C) obtained in alloy samples of NdFeB with additive elements (Al, Cu, Ga, Nb)

Alloy composition	B_r(T)	H_{ci}(kA/m)	H_k(kA/m)	H_k/H_{ci}	T_C(K)
36Nd–1.2B–Fe	1.22	710	650	0.92	585
36Nd–1.2B–1Al–Fe	1.07	820	660	0.8	570
36Nd–1.2B–1Cu–Fe	1.15	880	700	0.8	580
36Nd–1.2B–1Ga–Fe	1.18	820	750	0.92	590
36Nd–1.2B–1Nb–Fe	1.20	1050	980	0.94	585

boundaries and at the grain junctions. In Nb added alloy, the additional phase formed with the additive element is distributed within the grains as well. The delineation of the grain boundary in samples with Al or Ga becomes well marked when etched and viewed under an optical microscope In other words, the wettability and distribution of the low melting eutectic Nd-rich phase in the intergranular region are improved by the addition of these dopant elements.[14] On the contrary, the grain coarsening effect and the spread of the dark gray phase at the grain junctions, as observed from the optical micrograph of the Al added sample, seem to be the reason for the poor rectangularity of the intrinsic demagnetization curve in spite of improvement in H_{ci}. The stray field contribution around the nonmagnetic region, such as the Nd-rich phase at grain junctions, seems to be an important factor determining the shape of the demagnetization curve. The demagnetization behavior observed in the Cu added alloys could also be attributed to the coarse grain junctions as evidenced from its optical microstructure. Evolving an appropriate microstructure with uniform distribution of the minor phases to improve the demagnetization characteristics appears possible at a low dopant concentration in the alloy.[15]

The x-ray diffraction patterns of all the samples show the presence of the φ phase as the main phase. The occurrence of the η phase and the fcc Nd-rich phase has also been noticed. There is, however, no evidence of the additional phases formed in the alloy samples from their corresponding x-ray diffraction pattern.

The microprobe backscattered electron images of the samples and the x-ray map of minor elements are shown in Fig. 7. Also shown in Table II is the solubility of the minor element in different phases as obtained from EPMA using wavelength dispersive spectrometry.

The dopant element concentration in the φ phase is low but it is much higher in the Nd-rich phase and in the additional phase. The solubility of Al in the φ phase is significantly large followed by that of Ga, Cu, and Nb. The observed variation in the properties of B_r and T_C can be explained on the basis of the dissolved level of dopant element in the φ phase of the samples. Higher concentration levels of Al and Cu dissolved in the φ phase contribute to the significant fall in B_r and T_C while the minimum concentration level of Nb for the marginal or negligible fall in the same properties. Ga, in spite of exhibiting a relatively higher solubility, affects B_r but causes an increase in T_C, both marginally. The substitution of Ga for Fe in the j_1 site in the tetragonal crystal structure of $Nd_2Fe_{14}B$ has been reported to be the reason for the rise in T_C since it results in changing the negative exchange interaction of the three coordination atoms, viz. for j_1-k_1 and j_1-j_1 pairs, into positive exchange interaction.[23]

The complexity of the intergranular region increases with additive elements. At least one additional phase is clearly identified in each of the samples with elemental addition besides the other minor phases, viz. Nd-rich and η. In Al and Cu added samples this new phase corresponds to $Nd(Fe_{1-x}M_x)_2$ where M is Al or Cu and in the Ga added sample, it corresponds to $Nd_6Fe_{11}Ga_3$. In the Nb containing sample, the new phase appearing in the form of tiny particles, corresponds to NbFeB. The analysis of the new phases in the samples with additives is in general agreement with Fidler and Knoch[24] who have earlier reported two types of phases formed in alloy modified NdFeB, one being rare earth

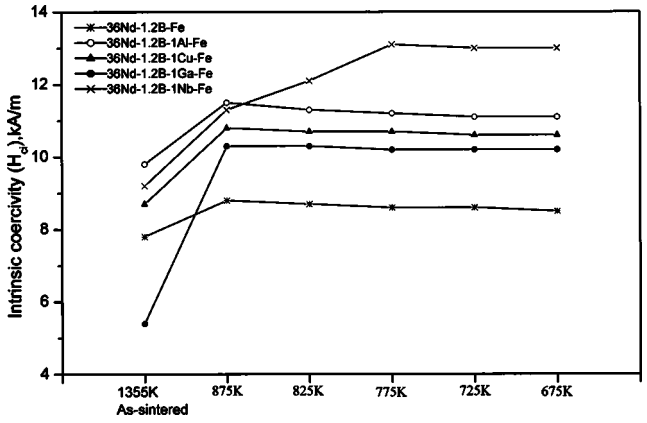

FIG. 3. Effect of heat treatment on the coercivity development in sintered samples of NdFeB with and without the addition of Al, Cu, Ga, and Nb.

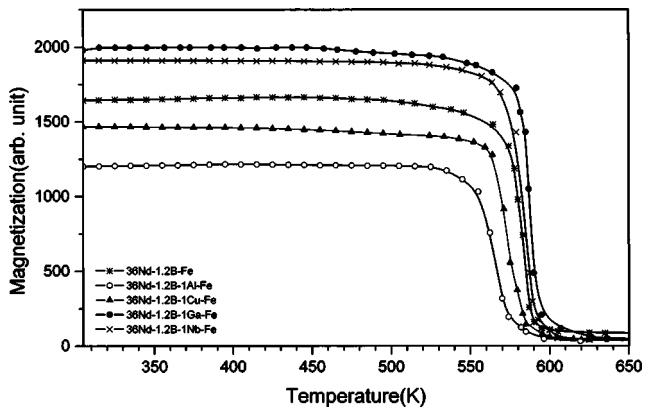

FIG. 4. Thermomagnetic plots of sintered NdFeB samples with and without additive elements, Al, Cu, Ga, and Nb.

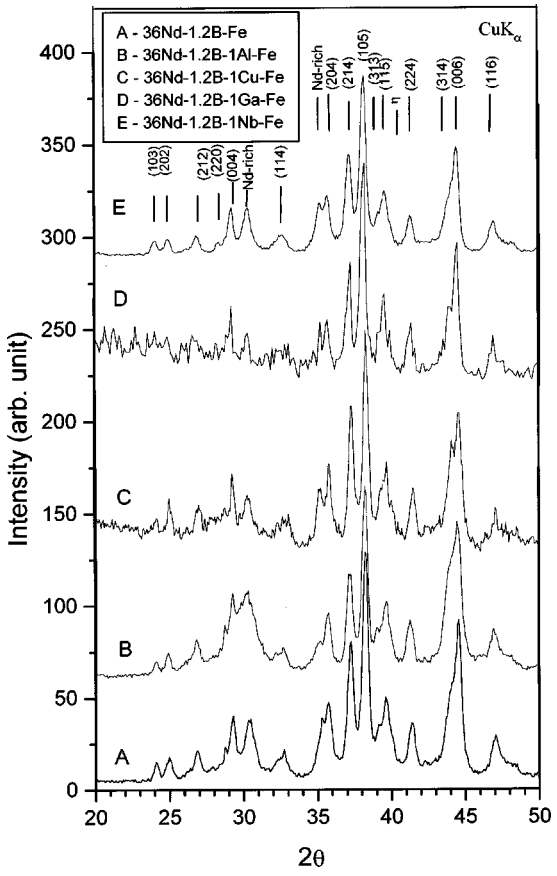

FIG. 5. X-ray diffraction patterns of sintered NdFeB magnet samples with and without additive elements, Al, Cu, Ga, and Nb. The patterns indicate the presence of three phases, viz. the φ phase, the η phase, and the Nd-rich phase.

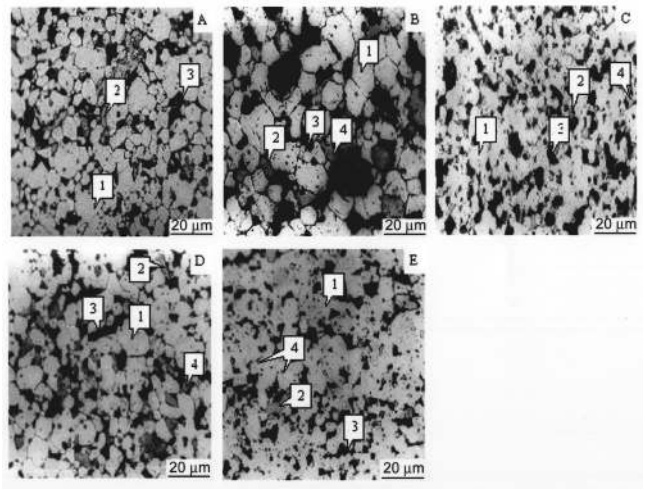

FIG. 6. Optical micrographs of sintered samples of (a) 36Nd–1.2B–Fe, (b) 36Nd–1.2B–1Al–Fe, (c) 36Nd–1.2B–1Cu–Fe, (d) 36Nd–1.2B–1Ga–Fe, and (e) 36Nd–1.2B–1Nb–Fe. The micrographs show the φ phase (1), η phase (2), Nd-rich phase (3), and a new phase with a high concentration of an additive element (4).

rich and containing a higher concentration of the minor elements such as Al, Ga, and Cu and the other being rich in transition metal (Fe) and containing the maximum concentration of the minor elements such as Nb, W, V, Ti, etc.

The ambivalence in the composition of the Nd-rich phase, noticeable strikingly in the ternary NdFeB, persists even in the alloys with additive elements. The Nd-rich phase exists in different concentration levels of Nd with varying solubility of Fe, an additive element, and possibly O and B, the last two of which could not be estimated.

The ability of Nb to form a compound with Fe in the NdFeB is viewed as beneficial for the development of high H_{ci} and also for the near rectangularity of the intrinsic demagnetization curve. Compositional shift and locally bound chemical inhomogeneity in the alloy during processing can lead to the formation of free Fe particles and they can act as easy nucleating centers for reverse domains to cause demagnetization of the magnet at a lower applied field. The suppression of Fe precipitation without consuming much of Nd is the main advantage arising from the addition of Nb to NdFeB. The improvement in H_{ci} towards a step-wise heat treatment with decreasing temperature, noticed in Nb added alloy, seems to indicate the pinning of the domain walls at the grain boundary; the pinning strength being a function of heat treatment temperature. The partial grain boundary separation seen in the optical micrograph of the Nb added sample also suggests that the boundary width is narrow for effecting domain wall pinning. A similarity in the grain boundary separation can be noticed even in the Cu added sample. However, due to the coarse size and distribution of the minor phases at the grain junctions, the stray field contribution for demagnetization is viewed to be high, which ultimately affected the second quadrant characteristics.

IV. SUMMARY AND CONCLUSIONS

The effect of the individual addition of Al, Cu, Ga, and Nb to NdFeB was studied. The demagnetization characteristics obtained for the samples after postsintering heat treat-

TABLE II. Solubility of additive elements (Al, Cu, Ga, Nb) in different phases coexisting in the sintered NdFeB alloy samples.

	Solubility of M in wt %				
Alloy composition 36Nd–1.2B–1M–Fe (M= Al, Cu, Ga, Nb)	φ phase	η phase	Nd-rich phase	Nd-rich phase with dissolved oxygen	New phase
36Nd–1.2B–1Al–Fe	0.5–0.7	<0.1	<1	0.3–2	1–3
36Nd–1.2B–1Cu–Fe	0.2 to 0.3	<0.1	<2	3–5	18–24
36Nd–1.2B–1Ga–Fe	0.3–0.5	~0.1	1–3	<0.2	15–18
36Nd–1.2B–1Nb–Fe	~0.1	<0.1	~0.4	<0.1	~50

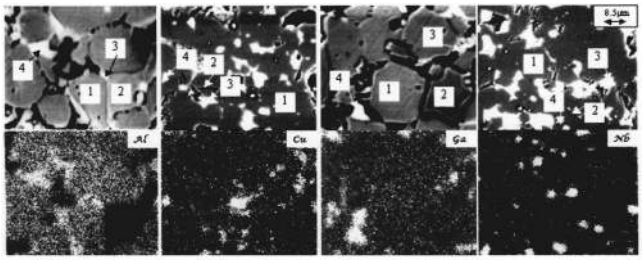

FIG. 7. Backscattered electron probe images of the sintered NdFeB samples with additive elements, Al, Cu, Ga, and Nb and the x-ray map of the corresponding dopant element showing its distribution in different phases: φ phase (1), η phase (2), Nd rich (3), and the additional new phase (4).

ment to realize the peak H_{ci} value were compared with the microstructural features viewed from optical and electron probe microanalysis. Following are the conclusions that emerged from the present study.

(1) H_{ci} enhancement is significant with Al, Cu, Ga, or Nb additions. Reduction in B_r and T_C is significant with Al or Cu addition. Nb and Ga additions show better demagnetization characteristics with a minimum change in T_C.

(2) Peak H_{ci} in sintered NdFeB samples can be reached with a postsintering heat treatment of 875 K/1 h but a step-heat treatment with decreasing temperature is suited for Nb added alloy. Pinning of the domain wall at the grain boundary by the Nb containing phase, with the pinning strength a dependent function of heat treatment temperature, is considered as a plausible reason for the H_{ci} improvement.

(3) The formation of at least one new phase is observed with each additive element to NdFeB. The concentration of the additive element in the new phase is high as compared to that in other phases.

The development of high H_{ci} in NdFeB depends on (i) the delineation of the grain boundary by the Nd-rich phase, (ii) the distribution of the minor phases in the intergranular region, especially in the grain junctions, since the coarse size configuration of the grain junctions, as observed in Al or Cu added alloys, may contribute to the rise of the stray field around them, impairing H_{ci}, and (iii) how the Nd-rich phase gets modified.

ACKNOWLEDGMENTS

The authors would like to thank DRDO, Ministry of Defense, Government of India for the financial support and the Director, DMRL, Hyderabad, India for the encouragement and permission to publish this work.

[1] D. Li, H. F. Mildrum, and K. J. Strnat, J. Appl. Phys. **57**, 4140 (1985).
[2] K. H. J. Buschow, D. B. de Mooij, S. Sinnema, R. J. Radwanski, and J. J. M. Franse, J. Magn. Magn. Mater. **51**, 211 (1985).
[3] H. Yamamoto, S. Hirosawa, S. Fujimura, K. Tokuhara, H. Nagata, and M. Sagawa, IEEE Trans. Magn. **MAG-23**, 2100 (1987).
[4] C. Lin, Z.-X. Liu, and X.-F. Xu, IEEE Trans. Magn. **MAG-23**, 2296 (1987).
[5] K. Fritz, J. Guth, B. Grieb, E.-T. Henig, and G. Petzow, Z. Metallkd. **83**, 11 (1992).
[6] M. Sagawa, S. Fujimura, H. Yamamoto, and K. Hiraga, IEEE Trans. Magn. **MAG-20**, 1584 (1984).
[7] M. Sagawa, S. Hirosawa, K. Tokuhara, H. Yamamoto, S. Fujimura, Y. Tsubokawa, and R. Shimizu, J. Appl. Phys. **61**, 3559 (1987).
[8] M. Sagawa and S. Hirosawa, J. Mater. Res. **3**, 45 (1988).
[9] H. Kronmueller, in *MRS International Meeting on Advanced Materials* (Materials Research Society, Pittsburgh, PA, 1989), Vol. 11, p. 3.
[10] D. Givord, P. Tenaud, and T. Viadieu, IEEE Trans. Magn. **MAG-24**, 1921 (1988).
[11] K.-D. Durst and H. Kronmueller, J. Magn. Magn. Mater. **68**, 63 (1987).
[12] W. Rodewald and W. Fernengel, IEEE Trans. Magn. **MAG-24**, 1638 (1988).
[13] X. C. Kou, X. K. Sun, Y. C. Chuang, T. S. Zhao, R. Grossinger, and H. R. Kirchmayr, J. Magn. Magn. Mater. **82**, 327 (1989).
[14] K. G. Knoch, B. Grieb, E-Th. Henig, H. Kronmueller, and G. Petzow, IEEE Trans. Magn. **26**, 1951 (1990).
[15] S. Pandian, V. Chandrasekaran, K. J. L. Iyer, and K. V. S. Rama Rao, IEEE Trans. Magn. **37**, 2489 (2001).
[16] S. F. H. Parker, R. J. Pollard, G. G. Lord, and P. J. Grundy, IEEE Trans. Magn. **MAG-23**, 2287 (1987).
[17] A. Kianvash and I. R. Harris, J. Appl. Phys. **70**, 6107 (1991).
[18] H. J. Engelmann, A. S. Kim, and G. Thomas, Scr. Mater. **36**, 55 (1996).
[19] G. F. Zhou, Z. C. Zhong, X. K. Sun, and Y. C. Chuang, J. Less-Common Met. **166**, 253 (1990).
[20] A. S. Kim, J. Appl. Phys. **63**, 3975 (1988).
[21] M. Tokunuga, H. Kogure, M. Endoh, and H. Harada, IEEE Trans. Magn. **MAG-23**, 2287 (1987).
[22] S. Pandian, V. Chandrasekaran, K. J. L. Iyer, and K. V. S. Rama Rao, J. Mater. Sci. **36**, 5903 (2001).
[23] C. R. Quan, J. G. Zhao, Y. Z. Wang, L. Yin, B. G. Shen, Z. X. Cheng, Y. F. Cheng, and S. W. Niu, Phys. Rev. B **42**, 6697 (1990).
[24] J. Fidler and K. G. Knoch, J. Magn. Magn. Mater. **80**, 48 (1989).